Supporting Information

Using Metal Oxide Nanoparticle Interlayer to Efficiently Anchor Polysulfides at High Mass Loading S-Cathodes in Li-S Rechargeable Battery

Subhra Gope, Aninda J. Bhattacharyya[*]

Solid State and Structural Chemistry Unit, Indian Institute of Science, Bangalore-560012, India

[*]E-mail: anindajb@iisc.ac.in

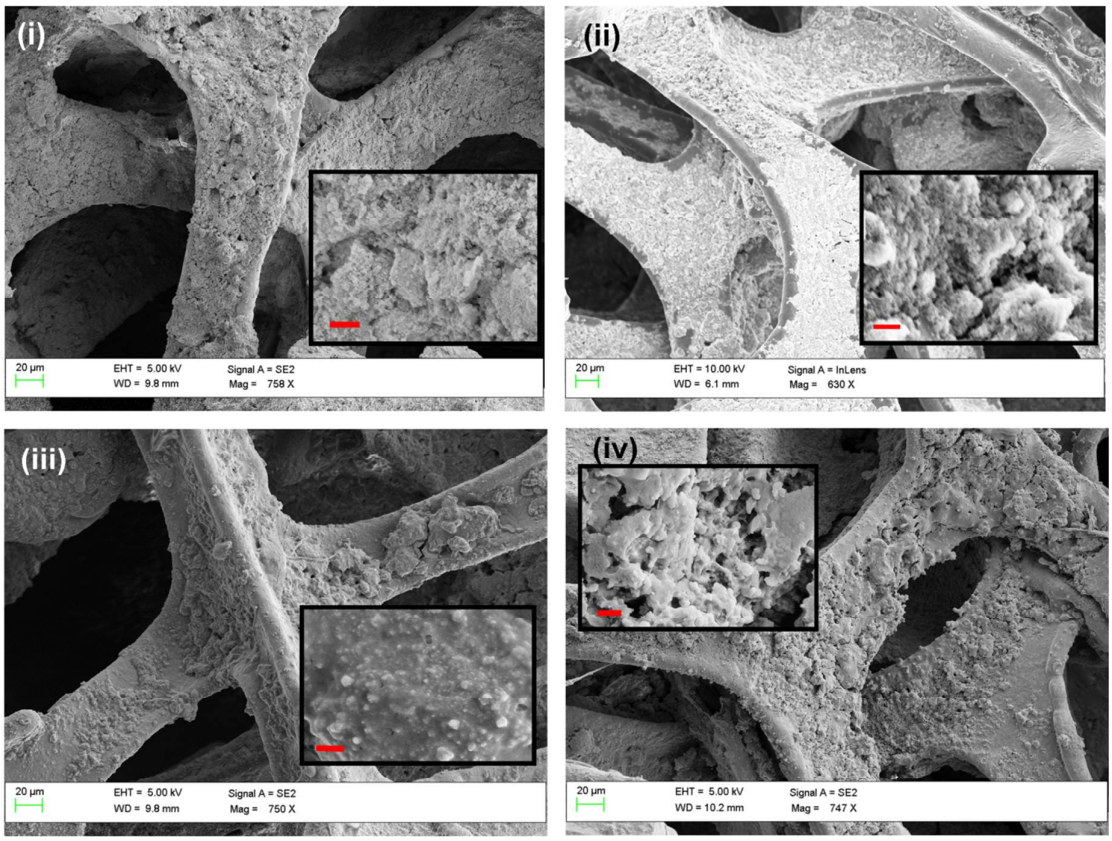

Figure S1: Low magnification SEM images of $Ni(OH)_2$-np (i) and NiO (ii) interlayers (nanoparticles deposited on Ni-foam) showing the even distribution of particles on Ni-foam substrate before cycling. Low magnification SEM images of $Ni(OH)_2$-np (iii) and NiO (iv) interlayers after cycling for 100 times in Li-S battery. (inset: magnified images of the interlayers at 1 µm scale shown by red line).

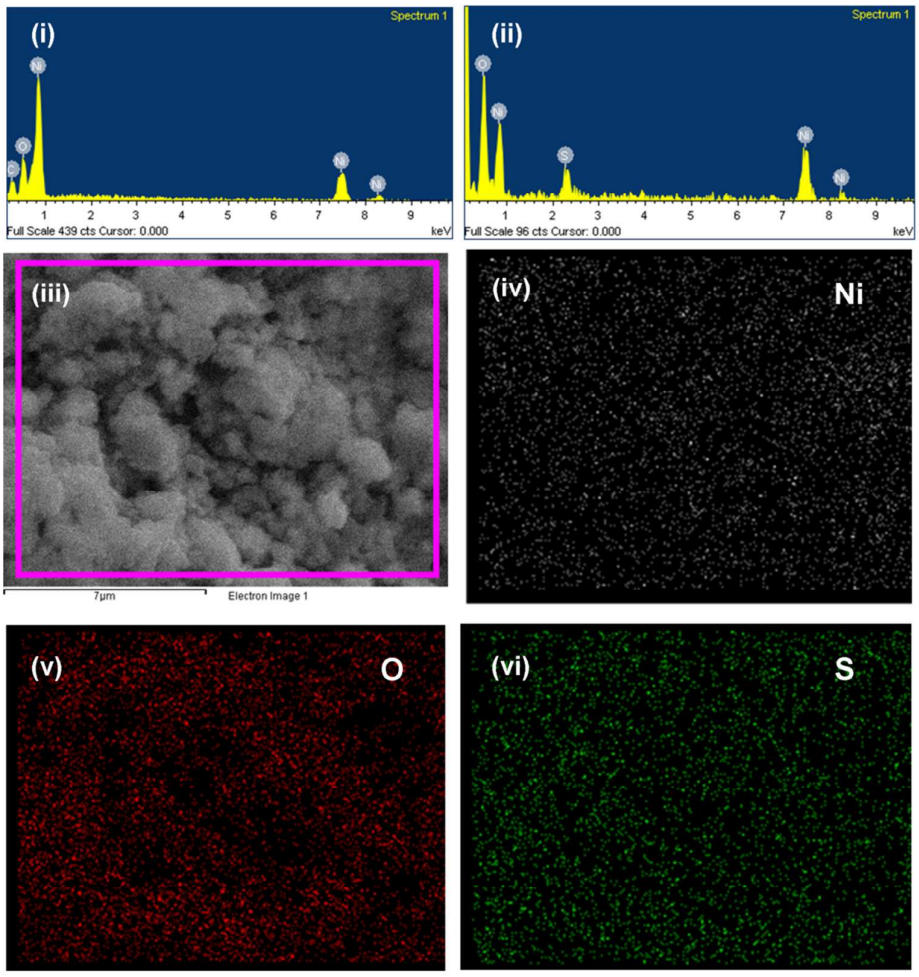

Figure S2 : EDS spectra of NiO (i) interlayer before cycling (ii) NiO interlayer after cycling. The spectrum obtained after cycling shows the presence of sulfur which is further verified by EDS mapping of the post-cycled NiO interlayer region shown in (iii). (iv-vi) Energy dispersive maps with respect to Ni, O and S respectively.

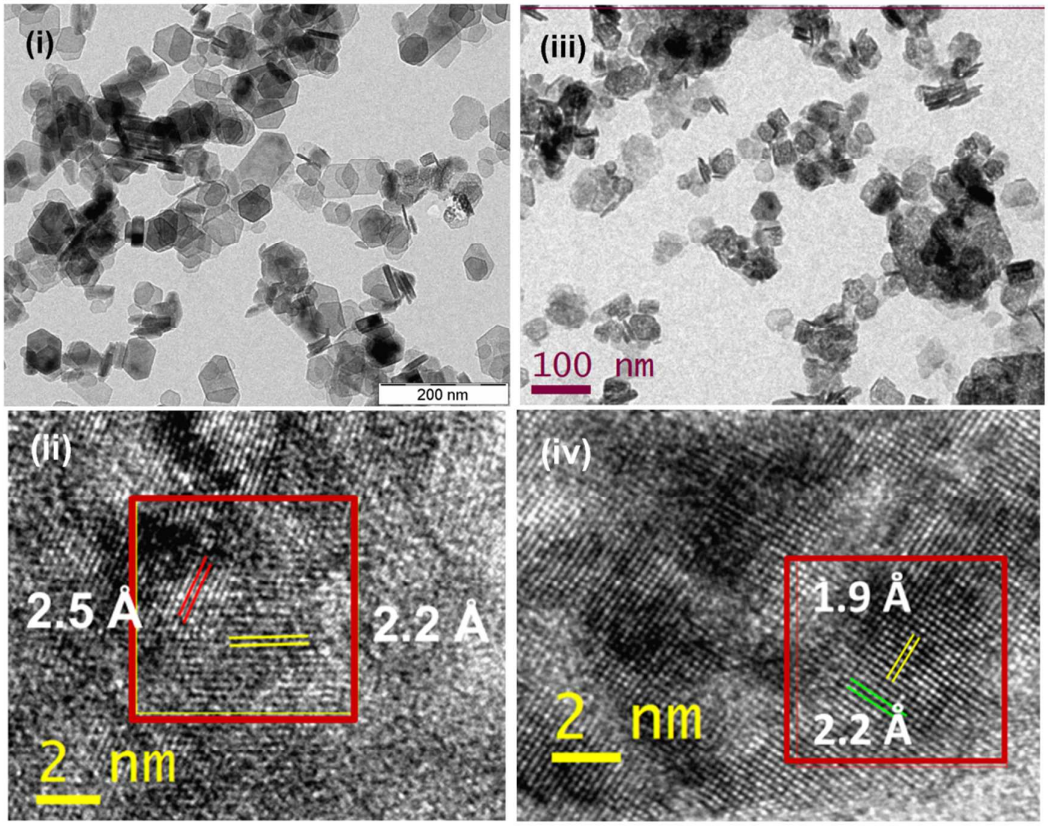

Figure S3: Low magnification TEM images of $Ni(OH)_2$-np (i) and NiO (ii) showing the even distribution of particle size with an average of 70 nm for $Ni(OH)_2$-np and 55 nm for NiO-np respectively. HRTEM of $Ni(OH)_2$-np (iii) and NiO-np (iv) showing the lattice spacing of the planes in respective samples.

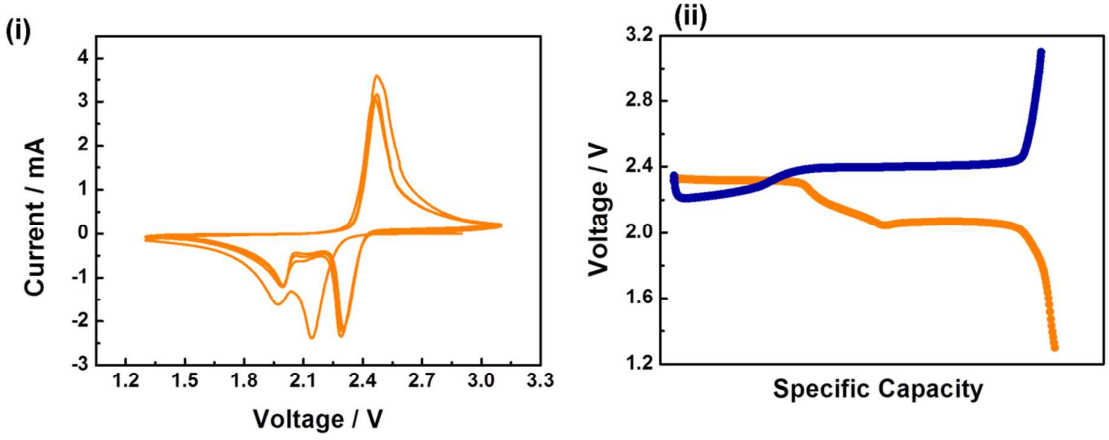

Figure S4: (i) Cyclic Voltammogram and (ii) an illustrative Galvanostatic charge-discharge curves, exhibiting usual discharge (yellow) and charge (blue) plateaus, of S/C cathode without using interlayer. Additional plateau as in case of the interlayers is absent in this case.

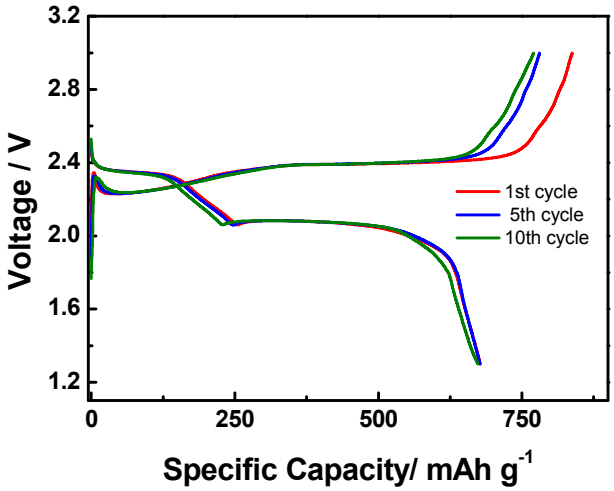

Figure S5: Galvanostatic charge-discharge cycle of an electrode with mass loading of 2 mg cm^{-2} with NiO interlayer.

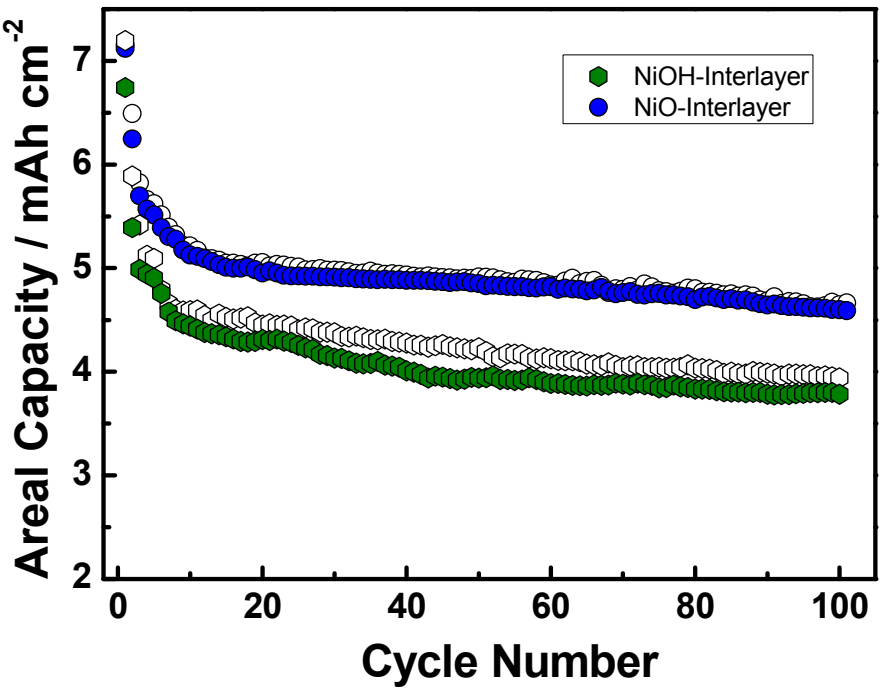

Figure S6: Areal capacity of Li-S battery for S/C cathode in presence of $Ni(OH)_2$-np (green) and NiO-np (blue) interlayers

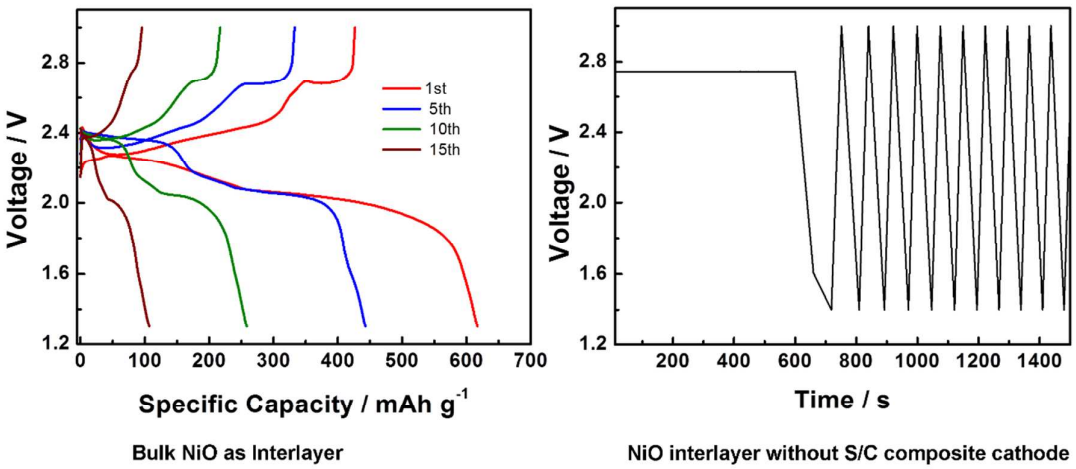

Figure S7: Galvanostatic cycling of S/C cathode with NiO-bulk interlayer (left panel), and NiO-np interlayer without S/C cathode (right panel).

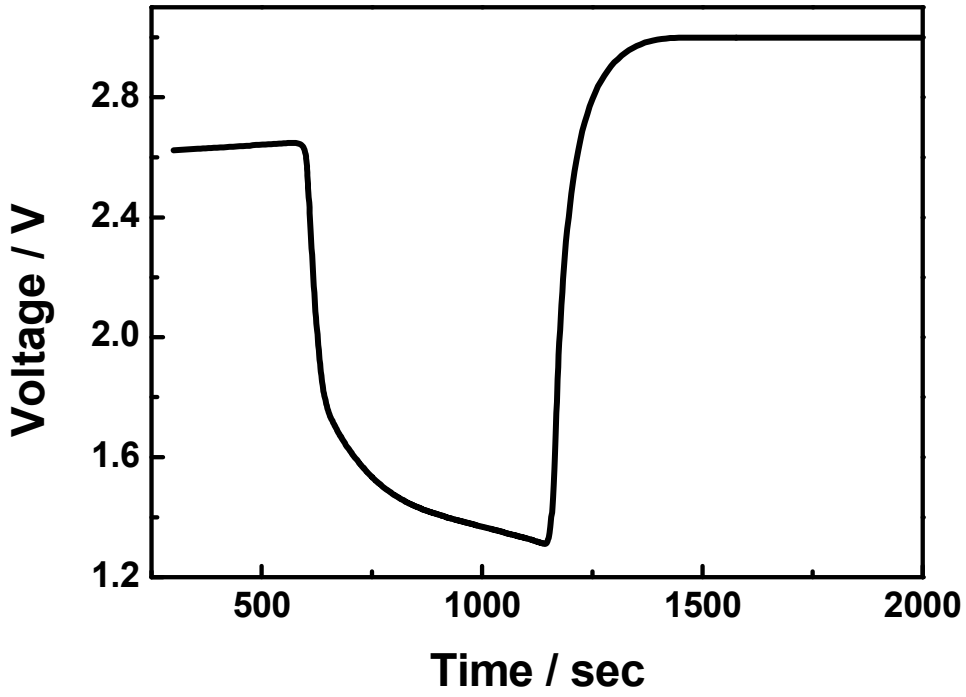

Figure S8: Galvanostatic cycling of S/C cathode with Ni-foam as the interlayer.

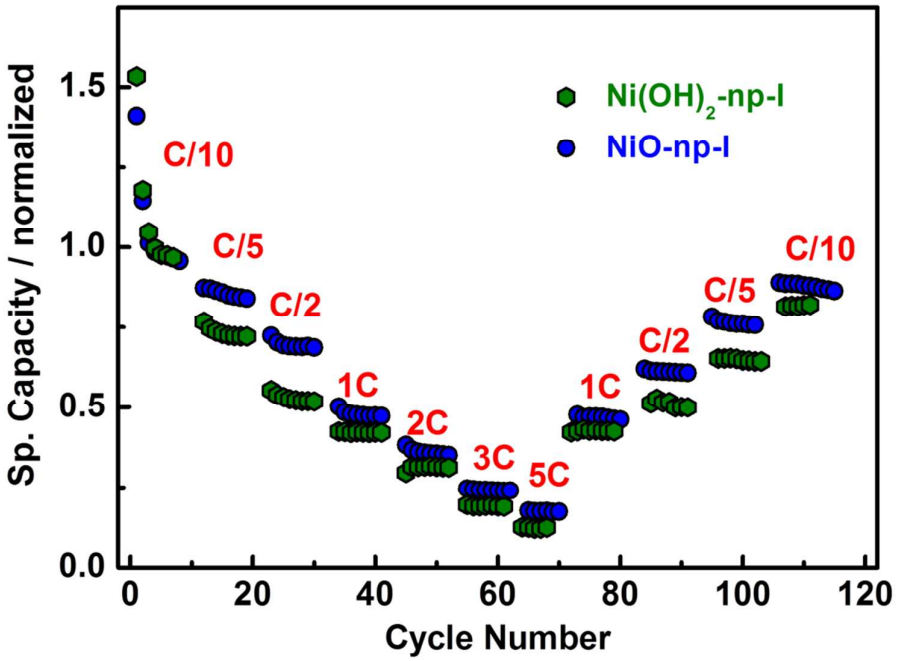

Figure S9: Rate capability performance of $Ni(OH)_2$-np (olive) and NiO (blue) interlayers with respect to the discharge capacities at 10^{th} cycle for the respective battery cycles at C/10 (ref. to Figure 4(i) of the manuscript)

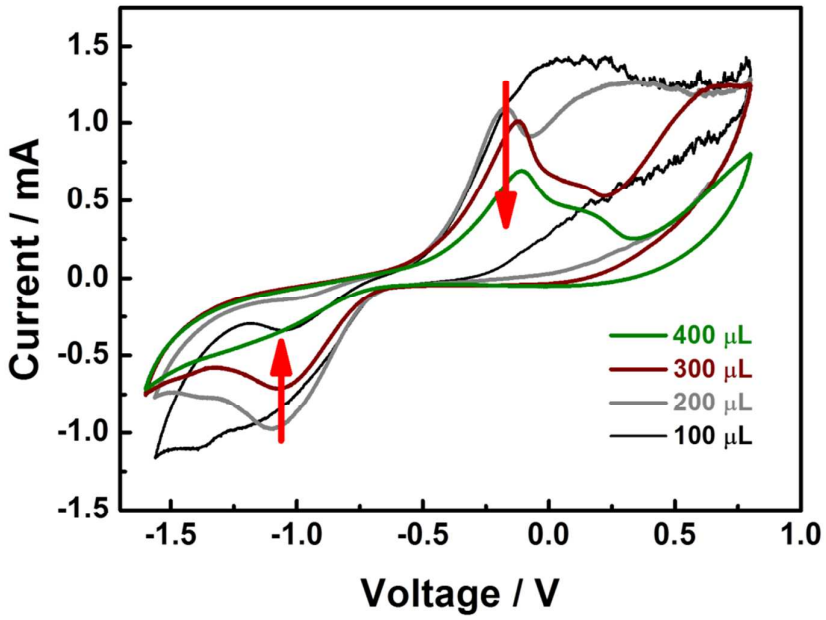

Figure S10: Cyclic voltammogram of polysulfide solution added to 1 M LiTFSI DOL-DME (1:1 v/v) solution in a three electrode system in presence of Ni-foam as working, Pt wire as counter and Calomel as reference electrodes, respectively exhibiting decrease in current response.

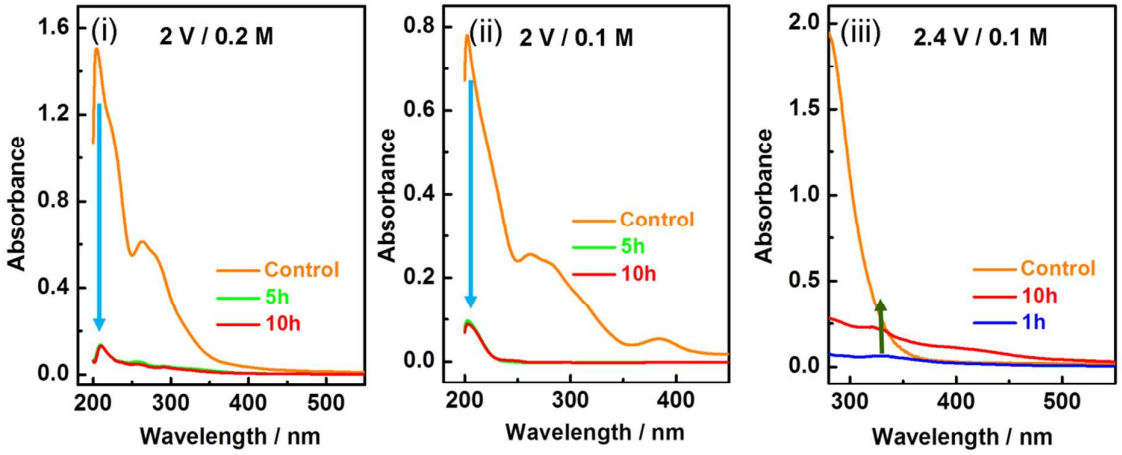

Figure S11: UV Absorbance measurement of 0.2 M (i) and 0.1 M (ii) polysulfide solution in 1 M LiTFSI DOL-DME (1:1 v/v) solution as electrolyte against NiO-np on Ni-foam subjected to chronoamperometry at 2 V exhibiting decrease in polysulfide concentration and (iii) at 2.4 V exhibiting increase in concentration of lower order polysulfide with time. The absorbance has been normalized with respect to the mass of NiO-np loaded on Ni-foam in all these cases.